# Corrosion of Low Pressure Steam Turbine Components

*Technical Report*

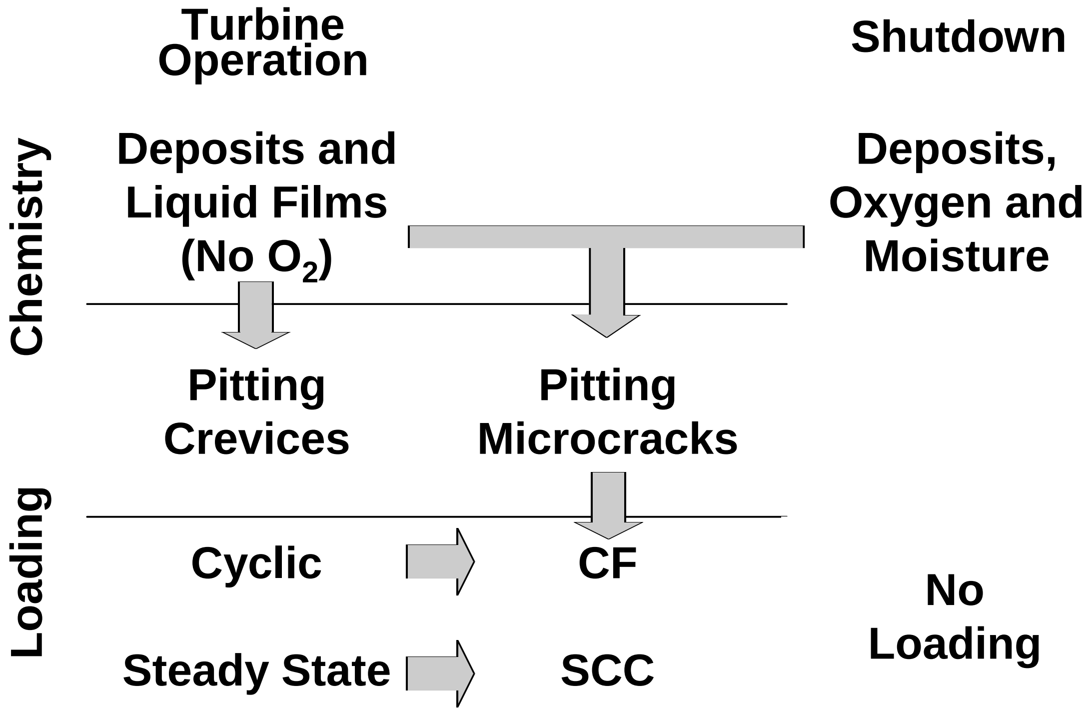

# Corrosion of Low Pressure Steam Turbine Components

**1000557**

Interim Report, November 2000

EPRI Project Manager
B. Dooley

EPRI • 3412 Hillview Avenue, Palo Alto, California  94304 • PO Box 10412, Palo Alto, California  94303 • USA
800.313.3774 • 650.855.2121 • askepri@epri.com • www.epri.com.

# DISCLAIMER OF WARRANTIES AND LIMITATION OF LIABILITIES

THIS DOCUMENT WAS PREPARED BY THE ORGANIZATION(S) NAMED BELOW AS AN ACCOUNT OF WORK SPONSORED OR COSPONSORED BY THE ELECTRIC POWER RESEARCH INSTITUTE, INC. (EPRI). NEITHER EPRI, ANY MEMBER OF EPRI, ANY COSPONSOR, THE ORGANIZATION(S) BELOW, NOR ANY PERSON ACTING ON BEHALF OF ANY OF THEM:

(A) MAKES ANY WARRANTY OR REPRESENTATION WHATSOEVER, EXPRESS OR IMPLIED, (I) WITH RESPECT TO THE USE OF ANY INFORMATION, APPARATUS, METHOD, PROCESS, OR SIMILAR ITEM DISCLOSED IN THIS DOCUMENT, INCLUDING MERCHANTABILITY AND FITNESS FOR A PARTICULAR PURPOSE, OR (II) THAT SUCH USE DOES NOT INFRINGE ON OR INTERFERE WITH PRIVATELY OWNED RIGHTS, INCLUDING ANY PARTY'S INTELLECTUAL PROPERTY, OR (III) THAT THIS DOCUMENT IS SUITABLE TO ANY PARTICULAR USER'S CIRCUMSTANCE; OR

(B) ASSUMES RESPONSIBILITY FOR ANY DAMAGES OR OTHER LIABILITY WHATSOEVER (INCLUDING ANY CONSEQUENTIAL DAMAGES, EVEN IF EPRI OR ANY EPRI REPRESENTATIVE HAS BEEN ADVISED OF THE POSSIBILITY OF SUCH DAMAGES) RESULTING FROM YOUR SELECTION OR USE OF THIS DOCUMENT OR ANY INFORMATION, APPARATUS, METHOD, PROCESS, OR SIMILAR ITEM DISCLOSED IN THIS DOCUMENT.

ORGANIZATION(S) THAT PREPARED THIS DOCUMENT

**SRI International**
**Pennsylvania State University**

# ORDERING INFORMATION

Requests for copies of this report should be directed to the EPRI Distribution Center, 207 Coggins Drive, P.O. Box 23205, Pleasant Hill, CA 94523, (800) 313-3774.

# CITATIONS

---

This report was prepared by

SRI International
333 Ravenswood Avenue
Menlo Park, California 94025

Author
G. Engelhardt

Pennsylvania State University
517 Deike Building
University Park, Pennsylvania 16802

Author
D. Macdonald

This report describes research sponsored by EPRI.

The report is a corporate document that should be cited in the literature in the following manner:

*Corrosion of Low Pressure Steam Turbine Components*, EPRI, Palo Alto, CA: 2000. 1000557.

# REPORT SUMMARY

---

Most outage hours for steam turbines are due to corrosion of low pressure (LP) blades and disks in the phase transition zone (PTZ). The development of an effective localized corrosion damage prediction technology is essential for the successful avoidance of unscheduled outages of steam turbines.

## Background

Over the last 10 years, EPRI and international collaborative work have described most aspects of the PTZ environment: moisture nucleation, early condensate composition, thickness and composition of liquid films on blade surfaces, deposition of salts on blade surfaces, and most recently the effect of charged droplets and liquid films. EPRI held a workshop on Corrosion of Steam Turbine Blading and Disks (TR-111340) to review the comprehensive information and to formulate the next stages. The development of a predictive modeling capability was recognized as being the central thrust.

## Objective

To develop an initial model for predicting the evolution of corrosion damage in PTZ components of the LP turbine.

## Approach

The project team developed the initial mathematical models for all stages in the initiation and propagation of corrosion damage: passivity breakdown, initiation of metastable pits, transition to stable pits, growth of stable pits, transition to a crack, growth of a subcritical crack, and final unstable fracture. During this process, the team identified two key areas of data deficiency, which need to be researched. EPRI has initiated this research. The project team has completed the development of the prototype models, which in the next stage of the work need to be optimized and tested.

## Results

The key results of this preliminary stage of the work can be summarized as follows:

- the model's overall structure has been developed and includes an overall damage module and modules for nucleation, growth, repassivation, and transition.
- an environment module provides the vital information on the environment of the liquid film on the blade/disk surface: composition, conductivity, thickness, corrosion potential, temperature, and mechanical conditions.

## EPRI Perspective

It is over 20 years since research was initiated to improve the understanding of processes in the salt zone, deposit buildup and behavior in the PTZ, and how these influence the major corrosion mechanisms. However, it is clear that these results have not led to a marked improvement in the overall reliability statistics of steam turbines. The initial development of the model represents the first step to bring together all the latest information on the PTZ, particularly the presence of liquid films during operation that have a potential and contain no oxygen. The model also will address the effects of unit operation and recognize that pitting can initiate during unprotected shutdown conditions. Once reliable electrochemical data for oxygen, hydrogen, and water reduction—along with values for the passive corrosion current density—are determined in the EPRI parallel research, they will be incorporated into the model. The next step will be to test the model on real corrosion situations. Ultimately, it is anticipated that this model for corrosion fatigue and stress corrosion cracking of LP turbine components will be incorporated into EPRI's BLADE code and ChemExpert.

## Keywords

Power plant availability
Steam turbines
Steam chemistry
Corrosion
Moisture
Pitting

# ABSTRACT

In this research, deterministic models and associated computer codes have been developed for predicting the evolution of corrosion damage in low pressure (LP) steam turbine blades. Mathematical modeling is based on the mechanistic/deterministic description of all stages in the propagation of corrosion damage, including passivity breakdown and the initiation of metastable pits, transition of metastable pits into stable pits, growth of the stable pits, transition of a pit into a crack, growth of a subcritical crack, and finally unstable fracture. The evolution of damage is described in terms of the damage function (DF), which is the histogram of event (pit, crack) frequency (number per unit area) versus increment in depth for a given observation time. By calculating the DF for increasing observation time, over which the operating conditions in the plant may change (e.g., shutdowns and startups), it is possible to determine the time at which the deepest event exceeds a critical dimension for the onset of unstable, fast fracture. This time corresponds to the failure time, and in general is a sensitive function of the operating history of the turbine.

The principal results of this investigation to date can be summarized as follows:

1. A differential equation for calculating the damage function (DF) has been derived. By analytical or numerical solution of this equation it is possible to calculate DF in complicated systems with different corrosion events (active and passive pits, stress corrosion cracking, corrosion fatigue, etc.) if the rate of nucleation, rate of propagation, and probability of survival of corrosion events are known.

2. A general mathematical model and corresponding computer code for calculating potential and concentration distributions in cavities for the cases of pitting corrosion, stress corrosion cracking (SCC) and corrosion fatigue (CF) has been developed. Mass transfer by diffusion, migration, and advection (fluid movement induced by the movement of the crack walls), anodic and cathodic processes at the crack tip and on the sides of the cavity, and hydrolysis and saturation solubility reactions is included in the model. The model also takes into account the potential drop in the external environment (outside the cavity).

3. On the basis of the general model, a simple approximate, but nevertheless rather accurate analytical model for calculating potential and concentration distributions along with cavity propagation rates has been developed for pitting corrosion and stress corrosion cracking. The model is based on the assumption that only those ionic species that are present at the highest concentrations in the crevice determine the potential distribution down the crack. The advantage of this method is that it permits simplification of the mathematics and allows one to predict the potential and concentration distributions without knowing various parameters, such as the equilibrium constants for homogeneous chemical reactions and the kinetic

parameters of electrochemical reactions that do not significantly change the concentrations of principal ionic species in the cavity. The fact that reliable analytical expressions can be obtained for the rate of pit or crack propagation is very important, because the accurate numerical simulation of the evolution of localized corrosion damage over a long turbine operating period may require a prohibitively large amount of computer time.

4. For the case of active metal dissolution at the tip of a one-dimensional slot under corrosion fatigue conditions, Nusselt numbers as a function of two dimensionless parameters have been calculated. For this particular case, the crack propagation rate can be quickly estimated by interpolation using these functions.

5. New criteria for the nucleation of stress corrosion and fatigue cracks from corrosion pits have been developed. Thus, it is shown that if the environmental component of the crack propagation rate is comparable with the mechanical (creep) component of the rate, the transition from a pit into a crack occurs if: (1) the depth of the pit exceeds some critical length (where stress intensity factor, $\Delta K$ exceeds the threshold stress intensity factor, $\Delta K_{tr}$), and (2) the pit is passivated.

6. General algorithms and computer codes for predicting localized corrosion damage in steam turbines have been developed.

Much supporting EPRI work is being conducted in parallel to the current studies, and a description of the experimental studies being carried out at the Pennsylvania State University and at the Frumkin Institute of Electrochemistry, Russian Academy of Sciences, Moscow, Russia, is provided in this report. A detailed description of proposed future work is also included.

# CONTENTS

# LIST OF FIGURES

# LIST OF TABLES

# 1

# INTRODUCTION AND PROJECT OBJECTIVES

Corrosion fatigue (CF) and stress corrosion cracking (SCC) of major steam turbines components such a blades, discs, and rotors have been consistently identified among the main cases of turbine unavailability [1]. Particularly susceptible components include rotating blades in the phase transition zone of low-pressure turbines, which have historically been the leading cause of steam turbine unavailability for large fossil fuel plants. SCC of discs and corrosion fatigue of blades (and their attachments) in phase transition regions also affect nuclear generating stations. The economic impact is apparently even higher than in fossil units.

Accordingly, the development of effective localized corrosion damage prediction technologies is essential for the successful avoidance of unscheduled downtime in steam turbines (and other complex industrial and infrastructural systems) and for the successful implementation of life extension strategies. Currently, corrosion damage is extrapolated to future times by using various empirical corrosion or fracture mechanics models coupled with damage tolerance analysis (DTA). In this strategy, known damage is surveyed during each outage, and the damage is extrapolated to the next inspection period allowing for a suitable safety margin. It has been argued [2] that this strategy is inaccurate and inefficient, and that in many instances it is too conservative. Instead, it has been suggested that damage function analysis (DFA) is a more effective method for predicting the progression of damage, particularly when combined with periodic inspection. DFA is based upon deterministic prediction of the rates of nucleation and growth of damage, with particular emphasis on compliance of the embedded models with the natural laws. Although corrosion is generally complicated mechanistically, a high level of determinism has been achieved in various treatments of both general and localized corrosion, which can be used to predict accumulated damage in the absence of large calibrating databases.

The main principal objective of this project is to develop deterministic models and associated computer codes for predicting the evolution of corrosion damage (i.e., “integrated” damage) in steam turbine blades and attachments. It is assumed that early corrosion damage initiates in highly localized areas, most commonly in the form of corrosion pits. After nucleation, the corrosion events develop and pass through distinct stages as schematically indicated in Figure 1-1. It is evident, that to describe the accumulation of damage quantitatively, that each of the stages must be described in mechanistic/deterministic form: namely, initiation of metastable pits, transition of pits from metastable to stable form, growth of stable pits, transition of a pit into a crack, growth of a subcritical crack, and finally unstable fracture.

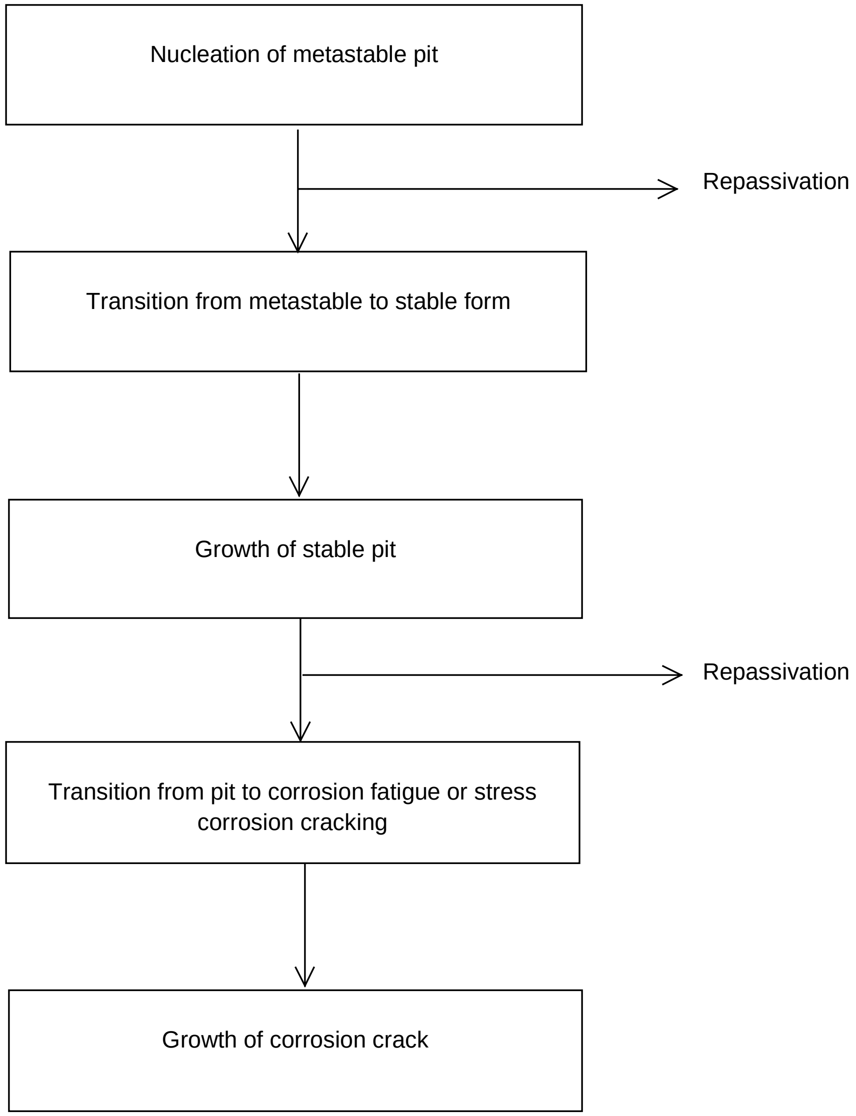

**Figure 1-1**
**Schematic history of the nucleation and propagation of corrosion damage**

Generally, the development of localized corrosion, in the general sense, is a *progressive* phenomenon, in which new damage nucleates while existing damage grows and dies. In the extreme, when all pits nucleate “instantaneously” (that is, within a time that is less than the time of first observation), the process is referred to as *instantaneous* nucleation and growth, and this form is commonly observed in systems that exist under very aggressive nucleation conditions. Under more benign conditions, such as those that exist in steam turbines, progressive nucleation and growth phenomena are expected to prevail, with the result that both the nucleation and growth processes must be described in statistical terms. However, stable pits and cracks that nucleate and grow on the surface are subject to “delayed” repassivation and hence die. Assuming that repassivation can be described as a rate process, which seems to be eminently reasonable, and if the repassivation process is kinetically first order (i.e., that the probability of repassivation is proportional to the number of active pits) then the rate of repassivation is described by a rate constant, $\gamma$. If the repassivation rate constant is greater than zero, all pits must eventually repassivate (i.e., they must "die") for sufficiently long observation times. However, some pits may grow to a sufficient depth before repassivation ("death") and can act as nucleation sites for cracks, projecting the system into an entirely different form of damage accumulation. Therefore, it is very important to obtain detailed information about the distributions of pits, cracks, and other defects in depth, or in other words, to determine the Damage Function (DF) of the system. It is also evident that quantitative calculation of DF is impossible without a quantitative description of the stage of repassivation of stable growing pits as is shown in Figure 1-1.

Below is described the current status of the project on developing quantitative, deterministic methods for predicting the accumulation of localized corrosion damage on stainless steel blades in low pressure steam turbines. The principal objective is to develop the capability for incorporation into EPRI's ChemExpert and within the EPRI BLADE Code for calculating the damage function for localized corrosion for any given observation time after a specified operating history (including startups, shutdowns and power cycling), with the specific purpose of calculating the failure time of the blade. The reason for this (DFA) approach is readily gleaned from the schematic damage functions shown in Figure 1-2.

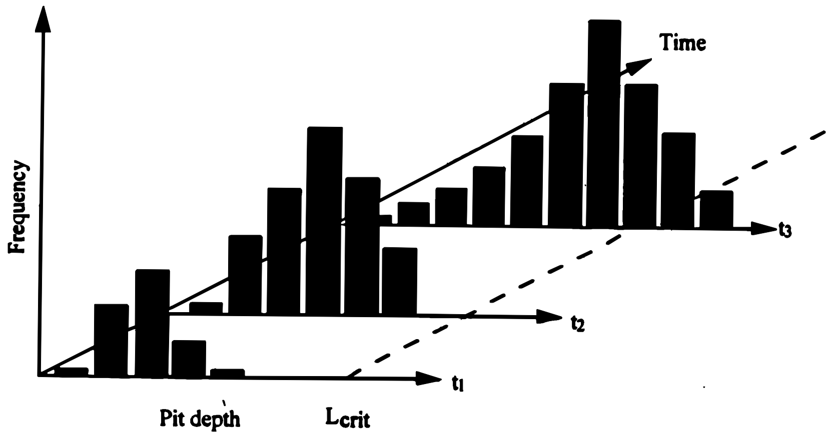

**Figure 1-2**
**Schematic of damage functions for localized corrosion as observed at three observation times ($t_1 < t_2 < t_3$).**

Thus, assuming a critical dimension of $L_{crit}$, corresponding to the crack length at which unstable (fast) fracture occurs for the prevailing loading conditions, it is evident that failure has not occurred at times $t_1$ and $t_2$ (see Figure 1-2). However, failure will have occurred at $t_3$, because only for this latter time does an event (pit or crack) have a depth greater than $L_{crit}$ (and hence $K_I > K_{IC}$).

The technology being developed in this program represents a radical departure from classical damage prediction methods, as noted above. However, many elements of the technology have been demonstrated previously, albeit in less sophisticated form, in predicting pitting corrosion damage in condensing heat exchangers [3] and stress corrosion cracking damage in BWR primary (liquid phase) coolant circuits [4].

Finally, one of the greatest challenges in the present project is to reduce the time of execution of the various component codes. This is necessary, because it will be necessary to perform hundreds of individual system simulations to model the accumulation of localized corrosion damage over a complicated operating history. Thus, a high execution speed is necessary to achieve acceptable accuracy and simulation times.

# 2

# CURRENT STATUS OF PROJECT

## 2.1 Damage Function Analysis

This project was begun by generalizing the Damage Function Analysis (DFA), which had been previously developed to predict localized corrosion damage in a number of related systems [1,2,5]. The problem is that the previous form of DFA was restricted to pitting corrosion alone, and hence was not directly extendable to the case of steam turbine blades, where at least one transition (from pitting to cracking) is observed. Moreover, it is possible that damage can initiate not only at corrosion pits, but also at other, highly localized sites, including: (1) fretting sites, (2) manufacturing defects, (3) microscopic surface imperfections, such as those produced by preferential dissolution of persistent slip bands or mechanical rupture of passive film due to slip dissolution, and (4) specific adsorption of species that locally reduce surface energy. That is why it is necessary to generalize DFA to the case where there are many different defect types on the steel surface and where the transition of one defect into another (e.g., pit into a crack) can occur. In addition, it is necessary to generalize DFA to recognize that the external environmental conditions in an operating turbine generally depend on time, which would allow a description, for example, of the accumulation of corrosion damage that occurs during the shutdowns and startups.

This goal has been addressed by expanding and generalizing the system of differential equations that describe the evolution of corrosion damage in the system. Localized corrosion damage in an arbitrary system is completely defined if it is known how many pits or other corrosion events (per $cm^2$) have depths between x and x + dx for a given observation time, t. Let this number be denoted by $f_k(x,t)dx$, where $f_k(x,t)$ is the so-called differential damage function (index k numerates different defects: active and passive pits, cracks, and so on). The simplest way for obtaining differential equations for damage functions is to use the following analogy.

The function, $f_k$, has dimensions of $\#/(cm^2\ cm) = \#/cm^3$ (like the concentration of a particle). Accordingly, it is very convenient to regard each defect as a "particle" that moves in the x direction (x=0 is at the metal surface with increasing x into the metal). The coordinate of this particle, x, coincides with the depth of penetration of the defect. Accordingly, $f_k$, can be regarded as the concentration of particles that must obey the law of mass conservation,

$$\frac{\partial f_k}{\partial t} + \frac{\partial j_k}{\partial x} = R_k, \qquad k = 1, 2, \ldots, K \qquad \textbf{Eq. 2-1}$$

where $j_k$ and $R_k$ are the flux density and the bulk source (sink) of the "particles" k, respectively, and K is the total number of corrosion defects.

It is evident that there is no “diffusion” mechanism for corrosion event transfer (corrosion defects can only grow), and, accordingly, $j_k$ can be presented in “convective” form as

$$j_k = f_k V_k \quad \textbf{Eq. 2-2}$$

where $V_k$, is the non-negative propagation rate for event k. Usually, but not always, $V_k$ is a function only of x. In some cases, $V_k$, can depend also on time, when external conditions (temperature, solution composition, corrosion potential, etc.) change with time or when the system exists under non-steady state conditions. Also, in “Darwinian” systems, where neighboring pits compete for the same resources and only the fittest survive, $V_k$ can depend on the “concentrations” of particles, i.e. on $f_k$ (nonlinear case).

This new formulation for DFA provides considerable advantage over the previous treatment: there now exists a method for calculating the DF for a complicated system. To fulfill this task, the system of Equations (2-1) and (2-2) must be solved with the corresponding boundary and initial conditions:

$$V_k f_k = n_k(t) \quad \text{at } x = 0, t > 0 \quad \textbf{Eq. 2-3}$$

and

$$f_k = f_{k0}(x) \quad \text{at } t = 0 \quad \textbf{Eq. 2-4}$$

where $f_{k0}(x)$ is the initial distribution of defect k [usually it can be assumed that $f_{k0}(x) = 0$)] and $n_k(t)$ is the velocity of nucleation of the same defect, i.e, $n_k(\tau)d\tau$ is the number of stable defects (per $cm^2$) that nucleate in the induction time interval between $\tau$ and $\tau + d\tau$.

This approach also shows that, for the theoretical prediction of damage in corrosion systems, the following set of four functions must be known (or calculated): the defect nucleation rate, $n_k(t)$; the rate of defect propagation, $V_k$, the repassivation rate, $P_k$, and the rate of transition of one defect into another, $R_k$.

In the early phases of this program, a highly efficient computer code was developed for the numerical solution of Equations (2-1) –(2-2) for the arbitrary functions $n_k(t)$; $V_k$, and $R_k$ using the finite difference method. An analytical solution has been obtained to Equations (2-1) for the important, particular case of the transition of a pit into a crack, when the rates of pit and crack propagation depend only on their depth and when the pit repassivation process obeys a first order decay law (see below).

## 2.2 Initiation of Metastable Pit

In accordance with the Point Defect Model (PDM) for passivity breakdown [6-10], the rate of nucleation of metastable pits, $n_{MP}$, as a function of induction time, $\tau$, is given by the following expression:

$$n(\tau)_{MP} = N_0 \frac{\exp\left[-\left(\frac{a}{\tau} + b\right)^2\right]}{\tau^2}$$ **Eq. 2-5**

where

$$a = \frac{\xi}{\sqrt{2}\sigma_D B},\ b = \frac{J_m}{\sqrt{2}\sigma_D B} - \frac{\overline{D}}{\sqrt{2}\sigma_D},\ \text{and}\ B = \frac{\chi F \varepsilon N_A a_x^{\chi/2}}{\Omega RT}\exp\left(\frac{\chi F(\beta pH + \alpha E_{corr}) + 2w}{2RT}\right).$$

In these equations, $N_0$ is the maximum number of metastable pits (per $cm^2$) that can nucleate on the metal surface. The definitions and detailed discussion of other parameters are available in the original papers [6-10]. The estimated values of these parameters for the corrosion of stainless steels and aluminum in chloride solutions can be found in References 5 and 11, respectively. It is important to note that parameters a and b depend on temperature (T), pH, activity of halide ion ($a_x$), and the corrosion potential ($E_{corr}$), but do not depend on the induction time ($\tau$).

As of now, the PDM recognizes only chloride adsorption as the trigger event for passivity breakdown. A start has been made to generalize the PDM to include cation ejection as an additional mechanism for passivity breakdown. For this purpose, attention has been focused on the case when interstitial cations are responsible (along with cation and oxygen vacancies) for charge transfer across the passive metal film. Mathematical methods and computer codes have been adapted or developed for solving the system of transport equations for ionic species and vacancies inside the thin passive film on the metal surface. This mathematical model recognizes that the film has moving boundaries (“Stefan” problems), due to dissolution of the oxide film at the film/solution interface and due to the oxidation of the metal at the metal/solution interface. These models allows calculation of distributions of interstitial cations, and of cation and oxygen vacancies in the film along with the film thickness, L, and the current density, I, when the applied voltage, V, is an arbitrary function of time, t. In some particular cases (short or long observation times), an analytical solution to the problem has been obtained. It has been shown that, for sufficiently thick oxide films, the diffusion of interstitial cations and of cation and oxygen vacancies in the film can be neglected, as compared with the migration of these species. The latter finding allows very simple analytical expressions for the concentrations of these species to be obtained, in both the steady state and under non-stationary conditions.

The possibility of calculating the polarization (current/voltage) behavior is very important, because it allows the parameters for the PDM to be obtained by comparing the model with experimental data that have been already obtained or will be obtained for Type 403 stainless steel later in this program. In turn, information on the PDM parameters will allow prediction of the probability and rate of pit nucleation for the case of turbine blade corrosion. The necessary experimental measurements at the Pennsylvania State University and at the Frumkin Institute (Moscow) have been initiated in parallel EPRI projects.

## 2.3 Transition of Pit from Metastable to Stable Form

Although an extensive database does not exist, it is postulated that the rate of nucleation of stable pits, n, is related to the rate of nucleation of metastable pits, $n_{MP}$, by

$$n = \lambda n_{MP} \tag{Eq. 2-6}$$

where $\lambda$ is the survival probability of a metastable pit. Note that the function n serves as a boundary condition for the equation for determining the damage function of the system. As of now, potentiostatic current-time transients are used for the experimental measurement of parameter $\lambda$ [11, 12]. The transients comprise fluctuations (peaks) superimposed on a background current, which may be rising, decreasing, or constant. The fluctuations may have a characteristic form of either a slow rise followed by a sharp fall [12] or of the opposite form (sharp rise and slow fall) [13]. The initiation frequency of the events, $\lambda$, can be obtained by counting the number of peaks in the current transient prior to the nucleation of a stable pit. In so doing, however, a problem may arise in deciding what is a significant peak and what is the background noise level in the electronic circuit (in the measuring system).

In order to obtain the reliable data for the survival probability of a metastable pit on Type 403 SS (turbine blade material), experimental measurements have been initiated at the Frumkin Institute (Moscow). It is expected that reliable results will be obtained in the beginning of 2001. Preliminary results show that survival probability is less than $10^{-2}$ (i.e., less than one in one hundred metastable events result in a stable pit).

## 2.4 Repassivation of Stable Pits

At the current time, it is assumed that pit repassivation obeys a first order decay law, which yields the following expression for the bulk source of passive pits and sink of the active pits in Equation (2-1)

$$R_p(x,t) = -R_a(x,t) = -\gamma f_a(x,t) \tag{Eq. 2-7}$$

where $f_a(x,t)$ is the differential damage function for active pits and $\gamma$ is the delayed repassivation ("death") constant. It is proposed to determine the constant $\gamma$ by fitting the theory to experimentally measured integral damage functions obtained for different $[Cl^-]$, pH, and voltage values [5]. By definition, the integral damage function

$$F_k(x,t) = \int_x^{\infty} f_k(x',t)dx' \tag{Eq. 2-8}$$

is the number (per $cm^2$) of pits (or cracks) with depth larger than x for a given observation time, t. This function can be determined by direct microscopic observation using a stereomicroscope to focus on the pit mouth and the pit base (if sufficiently open), by preparing a replica using dentist's molding compound, or by machining away the surface layer-by-layer and counting the remaining pits. Experimental measurements of the death constant, $\gamma$, on the Type 403 SS have been initiated at the Frumkin Institute (Moscow). It is expected that reliable experimental results will be obtained in the near future.

## 2.5 Transition from Pit to Crack

As concluded from experimental data [14], two conditions must be satisfied for crack nucleation to take place: $K_I > K_{ISCC}$ (for stress corrosion cracking, SCC), or $\Delta K_I > \Delta K_{I,th}$ (for corrosion fatigue, CF) and $V_{cr} > V_{pit}$, where $K_I$ and $K_{ISCC}$ are the stress intensity and critical stress intensity factors, respectively. $\Delta K_I$ and $\Delta K_{I,th}$ are the corresponding parameters for corrosion fatigue, while $V_{cr}$ is the crack growth rate. The first requirement defines the mechanical (fracture mechanics) condition that must be met for the prevailing stress and geometry, while the second simply says that the nucleating crack must be able to “out run” the pit. However, in accordance with the slip dissolution model, the crevice tip is partially blocked by the passive film. Accordingly, for a given set of tip conditions (metal potential, pH, etc.), the anodic dissolution rate of the crevice tip must be smaller (estimations show that it must be much smaller) than the pit propagation rate (with the bare tip surface). This means that, if the environmental component of the crevice propagation rate, $V_{env}$, is comparable to the mechanical component of the rate, $V_{mec}$, (i.e. when environmental effects play a role), the transition from a pit into a crack occurs if:

1. The depth of the pit exceeds some critical length, $x_{mec,}$ (where $K_I \geq K_{ISCC}$ for SCC or $\Delta K_I \geq \Delta K_{I,th}$ for CF),

and

2. The pit is passivated (when pit propagation rate, $V_{pit}$, is very small).

This new criterion for the transition of a pit into a crack (i.e., that cracks nucleate from “dead” pits) has been used for calculating the damage function of the system. It is important to emphasize that the old theory, which did not take into account the impact of repassivation on cavity growth rate, was unable to explain the transition of a pit into a crack except by purely “hand waving” means. Additionally, the old theory yields an absolutely different expression for the damage function for SCC. Thus, in accordance with the old theory, the transition from a pit to a crack definitely occurs when the depth of the pit increases above some critical value, $x_{tr}$. However, it is now required that, for $x > x_{tr}$, both conditions ($K_I > K_{ISCC}$ for SCC, or $\Delta K_I > \Delta K_{I,th}$ for CF, and $V_{cr} > V_{pit}$) must hold. Accordingly, it can been shown that the damage function for cracks, $f_{cr}$, for this system has the form

$$f_{cr}(x,t) = \exp[-\gamma\, \theta_{pit}(x_{tr})]\, n[t - \theta_{pit}(x_{tr}) - \theta_{cr}(x, x_{tr})] \text{ at } x > x_{tr} \qquad \textbf{Eq. 2-9}$$

where

$$\theta_{pit}(x) = \int_0^x \frac{dx'}{V_a(x')} \quad \text{and} \quad \theta_{cr}(x, x') = \int_{x'}^x \frac{dx''}{V_{cr}(x'')} \qquad \textbf{Eq. 2-10}$$

are the ages of an active pit having depth x, and a crack with the depth x, which was born at the distance x′ from the metal surface, respectively. For x <$x_{tr}$, then simply $f_{cr}(x,t) = 0$. In accordance with the new transition criteria, the pit will transition into a crack only when its depth increases to some value, $x_{mec}$, where conditions $K_I > K_{ISCC}$ for SCC, or $\Delta K_I > \Delta K_{I,th}$ for CF, and $V_{cr} > V_{pit}$ hold. The pit can transition into a crack only if it is passivated at $x > x_{tr.}$ It can be shown that DF for the crack, for this case, has the form

$$f_{cr}(x,t) = \frac{\gamma}{V_{cr}(x)} \int_{x_{mec}}^{x} f_a\left[x', t - \theta_{cr}(x,x')\right] dx' \text{ at } x > x_{mec} \qquad \textbf{Eq. 2-11}$$

where

$$f_a = \frac{\exp[-\gamma\theta(x)]\, n[t - \theta(x)]}{V_a(x)} \qquad \textbf{Eq. 2-12}$$

is the damage function for active pits. For x < $x_{mec}$, we have $f_{cr}(x,t) = 0$. The difference between the two damage functions [see Equations (2-9) and (2-11)] becomes especially evident for small values of the repassivation constant, γ.

## 2.6 Pit and Crack Propagation Rate

The quantitative description of pit and crack growth can be regarded as one of the key problems in predicting corrosion damage in many practical systems. This follows from the fact that the calculated corrosion damage that is based only on this stage can be compared with experiment, in many limiting cases. For example when all pits nucleate "instantaneously", or when the induction time of pit nucleation is much smaller than the observation time, it is possible to ignore the initial stage of pit nucleation. In addition, if the probability of survival of the corrosion defect is sufficiently high (as for stress corrosion cracking), the possibility that a corrosion defect nucleates immediately after the start of plant operation and propagates without repassivation must be taken into account. In any case, calculations based only on the growth stage yield the most conservative estimate of the service life, $t_{s,min}$, of the turbine. If the calculation of service life based on growth alone is made properly, then the real service life, $t_s$ will at least not be less than $t_{s,min}$.

A general mathematical model and corresponding computer code for calculating potential and concentration distributions in corrosion cavities (pits and cracks) has been developed. Calculational procedures reduce to solving the relevant system of mass conservation equations for the species in the solution. It can be shown that, if the width of the cavity, w, is much smaller than the crack depth, L, then averaging between the walls of the crack yields transport equations of the form:

$$\frac{\partial(wC_k)}{\partial t} = \frac{\partial(wN_k)}{\partial x} = wR_{Vk} + 2N_{sk}, \qquad k = 1,\ldots,K \qquad \textbf{Eq. 2-13}$$

where $N_k$ is the flux density, $R_{Vk}$ is the rate of creation of ionic species, k, per unit volume, $N_{sk}$ is the flux of species k through the metal-solution interface on the side walls, and K is the total number of species.

Mass transfer by diffusion, migration, and convection, due to the movement of the crack walls, is considered and, according to dilute solution theory, the flux of species, k, is given by the Nernst-Planck equation:

$$N_k = -D_k\left(\frac{dc_k}{dx} + \frac{z_k F}{RT} c_k \frac{d\varphi}{dx}\right) + c_k v \qquad \textbf{Eq. 2-14}$$

where $c_k$ is the concentration of species k, $D_k$ is the diffusion coefficient, $z_k$ is the charge, T is the temperature, R is the gas constant, x is the distance down the crevice, and φ is the electrostatic potential. The fluid velocity, v, (averaged across the width of the crack) can be found from the equation for the conservation of mass for an incompressible liquid, and has the form:

$$v(x,t) = \frac{1}{w}\int_x^L \frac{\partial w}{\partial t} dx \qquad \textbf{Eq. 2-15}$$

The velocity is readily calculated if the function w(x,t) is known.

The solution within the crevice is taken to be electrically neutral, so that

$$\sum_k z_k C_k = 0 \qquad \textbf{Eq. 2-16}$$

It has been suggested that, in the mathematical simulation of the corrosion of steels in neutral solutions, at least six species in the solution must be taken into account [15]. These species are metal ions from the dissolution process, sodium and chloride ions (for example) that are commonly included to control the bulk conductivity, hydrogen and hydroxyl ions from the dissociation of water, and a metal hydrolysis product. For generality, oxygen species were also included in the model.

It was assumed that the homogeneous reactions of metal ion hydrolysis, hydrolysis product solubility, and the dissociation of water occur in the cavity. The cathodic reduction of hydrogen ion, water, and dissolved oxygen can take place on the metal surface, both within the crack (on the crack walls) and on the external surfaces. It is also assumed that the metal is in the active state at the tip of the crack and that a constant anodic passive current density, $i_P$, flows across the crevice walls. It is important to note that in previous models [16, 17] it is supposed that the metal on the sides of the cavity is in the state of active anodic dissolution, i.e. in the same state as that at the tip of the crack. This means that the electrochemical reaction at the crack tip does not visibly influence the potential and concentration distributions, because the area of crack tip is much smaller than the area of crack sides. Furthermore, it is difficult to account for the persistence of a sharp crack geometry on the basis of this assumption. However, it is much more realistic to assume that the sides of cracks in stainless steel turbine blades are in the passive state (with a relatively small passive current density flowing through them). As follows from experimental data and Faraday's law, the average current density of metal dissolution at the crack tip is much greater than that on the passive sides, and hence the crack remains sharp. The crack tip current density depends on the crack strain rate, which in turn is the function of applied load [18]. That is why the influence of mechanical variables on the average current density at the crack tip must be included in any model when quantitatively describing corrosion fatigue in steam turbines.

The second very important issue that differentiates this model from previous models is that this model also takes into account the potential drop in the external environment (outside the cavity). This issue is very important for the case of steam turbines, because the bulk concentration of impurities in an electrolyte can be very low and/or because the electrolyte film is very thin. Accordingly, a large potential drop exists in the external environment (outside the crack), requiring that the transport processes in the internal and external environments be coupled by charge conservation [19] when constraining the solutions to the problem. As noted above, this potential drop can be very high if the thickness of the electrolyte film, h, is sufficiently small, and corrosion must even stop if the thickness goes to zero (surface completely dries).

First the cases of pitting corrosion and stress corrosion cracking when v equals zero will be described. The corrosion fatigue case will be considered first, as presented below. Figure 2-1 shows calculated concentration distributions in a crevice having a depth equal to 1 mm. The bulk concentration of NaCl was chosen to be $10^{-5}$ M, which is a typical value for the electrolyte film on a steam turbine surface [20], provided that cyclical wetting and drying has not occurred. Furthermore, the steam environment was assumed to be deaerated. The average current density at the crack tip was taken to be $10^{-2}$ A $cm^{-2}$, which for dissolution-controlled crack growth yields a crack growth rate of about $3\times10^{-8}$ cm $s^{-1}$. Kinetic parameters for the chemical and electrochemical reactions were taken from reference 21.

Some important conclusions can be drawn on the basis of Figure 2-1. Perhaps the most important is that two species dominate in the crevice; $Fe^{2+}$ and $Cl^-$ (i.e., the electrolyte can be regarded as being binary) and only these species determine the electrostatic field in the cavity. Hence, to calculate the potential distribution in this system, the complete system involving seven species ($Fe^{2+}$, $Fe(OH)^+$, $Na^+$, $Cl^-$, $H^+$ $OH^-$, and $O_2$ ) can be approximated by a reduced system involving two species ($Fe^{2+}$, $Na^+$). In more concentrated NaCl solutions, $Na^+$ must be also taken into account.

The analytical solution for such a simplified system of transport equations for the case of deep pits and cracks has been developed and yields the following result for the average current density at the cavity tip:

$$i_{tip} = \frac{\bar{i}}{[1+\lambda\varsigma L\bar{i}/(z+1)]^{\alpha/(1+\alpha)}} \qquad \textbf{Eq. 2-17}$$

where $\alpha$ is transfer coefficient for the active metal dissolution reaction, $\varsigma = 1/(FD_1[Cl^-])$ , $D_1$ is the diffusion coefficient of metal ions, z is the oxidation charge of the metal (or effective charge for alloy dissolution), $[Cl^-]$ is the bulk concentration of chloride ion, $\bar{i}$ is the average current density for active metal dissolution calculated at $E_{mouth}$ (the metal potential near the crevice mouth), and $\lambda$ is a geometrical parameter. For cylindrical pits and one-dimensional slots, $\lambda = 1$. For trapezoidal crevices,

$$\lambda = -\frac{(1-\nu)}{\nu}\mathrm{Ln}(1-\nu) \qquad \textbf{Eq. 2-18}$$

where $\nu = (w_{mouth} - w_{tip}) / w_{mouth}$.

Finally, by taking into account Faraday's law, the sought after expression for the crack propagation rate as a function of crack depth, L is obtained:

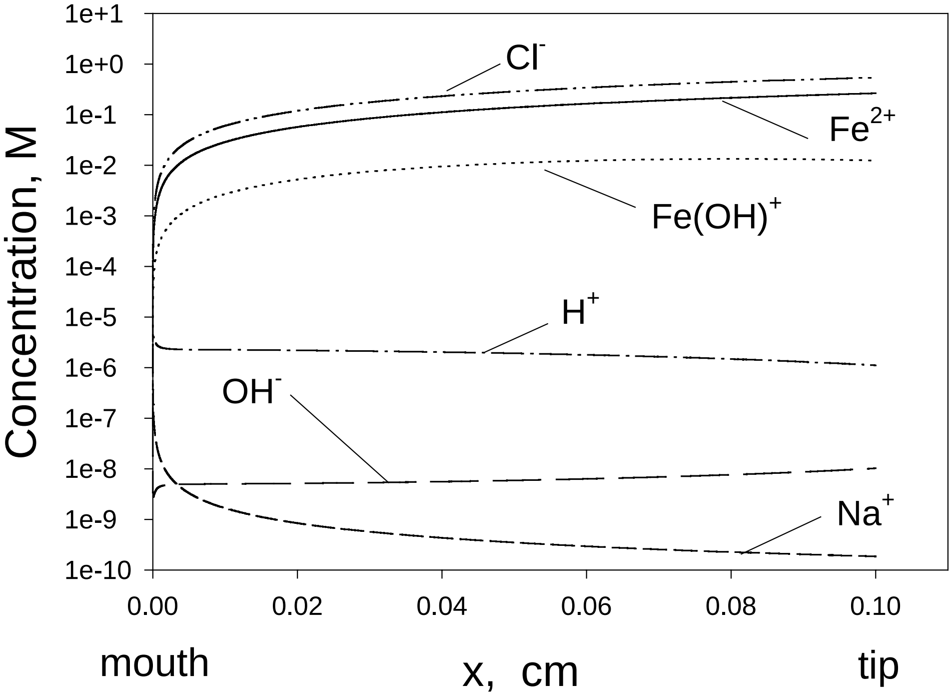

**Figure 2-1**
**Calculated concentrations of species down a crack**

$$\frac{dL}{dt} = \frac{Mi_{tip}}{z\rho F} \qquad \textbf{Eq. 2-19}$$

where M and $\rho$ are the molecular weight and the density of the metal, respectively, and $i_{tip}$ is described by Equation (2-17).

There is one particular problem that impacts the practical use of Equation (2-17). Thus, the parameter $\bar{i}$ must be calculated at a metal potential existing at the crevice mouth that, in general, differs from the corrosion potential of the system, $E_{corr}$. This is so, because a potential distribution exists in the external environment that results in the flow of positive (ionic) current from the crevice (pit or crack) mouth to the external surfaces, where it is consumed by the reduction of a cathodic depolarizer (e.g., $O_2$, $H^+$, and/or $H_2O$).

The general approach for solving such problems is to couple the transport equations inside and outside the cavity, such that the coupled system satisfies the law of charge conservation [19]. Because there is an analytical relation between the average current density at the crevice mouth, $i_{mouth}$, and the potential of the metal at the crevice mouth, $E_{mouth}$, yields a unique possibility to decouple the transport problem. This is because the above-mentioned relation can be regarded as a boundary condition for the external environment.

By averaging Laplace's equation for the electrostatic potential, a very simple analytical solution has been obtained that yields the ratio $\bar{i}/\bar{i}_0$, where $\bar{i}_0$ is the average current density of active metal dissolution calculated at the corrosion, $E_{corr}$, and which is supposed to be known. This analytical expression has the form:

$$\Omega \equiv \frac{\bar{i}}{\bar{i}_0} = \frac{1}{(1+A)^{\gamma/(\gamma+0.5)}} \qquad \textbf{Eq. 2-20}$$

where

$\gamma = \dfrac{1}{1+\alpha}$, $A = \dfrac{w_{tip}}{2\sqrt{2}h} \dfrac{\bar{i}_0}{[\lambda\varsigma L\bar{i}_0/(z+1)]^{\alpha/(1+\alpha)}} \sqrt{\dfrac{\alpha F i_p h \kappa}{RT}}$ , and $\kappa$ is the conductivity of the electrolyte film. Figure 2-2 illustrates the accuracy of Equation (2-20). After calculating $\bar{i}_0$ from Equation (2-19), the cavity propagation rate can be determined analytically by using Equations (2-16) and (2-18).

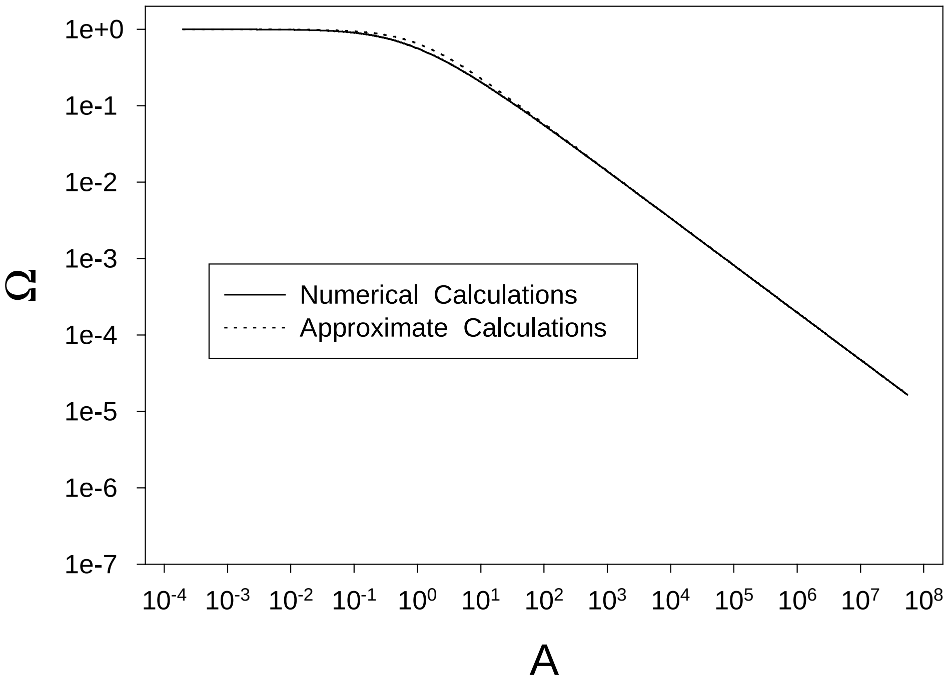

**Figure 2-2**
**Ratio of current density on active metal surface calculated at $E = E_{mouth}$ to the same value calculated at $E = E_{corr}$ as a function of the dimensionless parameter A for $\gamma = 1/(1+\alpha) = 0.675$.**

It is very important to note that, in spite of the fact that the above formula yields very accurate results (relative to numerical calculations), their applicability depends on accurate values being available for various electrochemical kinetic parameters for the anodic and cathodic reactions. These parameters for steam turbine Type 403 stainless steel can differ significantly from the kinetic parameters for carbon steels that were used in the present calculations. That is why it is very important to acquire direct experimental data for these parameters, especially for the passive corrosion current density and for the kinetic parameters for active metal dissolution for alloys that are used in steam turbine blades. The required data are currently being measured at the Pennsylvania State University and the Frumkin Institute (Moscow) in parallel EPRI projects.

The case of corrosion fatigue was investigated numerically, as was pitting corrosion and SCC. It was assumed that the specimen has the compact tension type of geometry, and that the crack geometry is trapezoidal with a width, w, defined by

$$w(x, t) = w_{tip}(t) + (L - x)\,\theta(t) \qquad \textbf{Eq. 2-21}$$

where $w_{tip}$ is the crack tip opening displacement (CTOD), and θ is the (small) crack angle, which is given by [22, 23]

$$\theta \approx \tan\theta = \frac{w_{mouth} - w_{tip}}{2L} = \frac{COD - CTOD}{2a} \qquad \textbf{Eq. 2-22}$$

Here, $w_{mouth}$ is the crack mouth opening displacement (CTOD), COD is the crack opening displacement at the loading line, and a is the crack length as measured from the loading line. The load is assumed to be sinusoidal, i.e. the stress intensity factor, $K_I$, is defined by

$$K(t) = K_m + \delta K \sin(2\pi ft) \qquad \textbf{Eq. 2-23}$$

where $K_m$ is the mean value of K, δK is the amplitude ( = 1/2ΔK, where ΔK is the range of K), and f is the cyclic frequency. CTOD and COD can be evaluated using the following expressions from Reference 23, which are based on the Dugdale-Balenblat [24] model and the compliance expression calibrated by Saxena [25] .

$$CTOD(t) = \frac{K^2(t)}{4E'\sigma_y} \qquad \textbf{Eq. 2-24}$$

and

$$COD(t) = \frac{K(t)W^{1/2}}{E'} \times \frac{Y'}{Y} \qquad \textbf{Eq. 2-25}$$

where $E'$ is the Young's modulus, $\sigma_y$ is the yield strength, W is the distance of the loading line to the base of specimen, and

$$Y = \frac{2 + a/W}{(1 - a/W)^{3/2}} \left[0.886 + 4.64(a/W) - 13.32(a/W)^2 + 14.72(a/W)^3 - 5.6(a/W)^4\right] \qquad \textbf{Eq. 2-26}$$

and

$$Y' = \left(\frac{1 + a/W}{1 - a/W}\right)^2 \left[2.163 + 12.219(a/W) - 20.065(a/W)^2 - 0.9925(a/W)^3 + 20.609(a/W)^4 - 9.9314(a/W)^5\right]$$

**Eq. 2-27**

In addition, it is assumed that the kinetics of the dissolution reaction at the crack tip, for a specific value of the stress intensity, are based on time-averaging the current density transient due to slip-induced fracture of the passive film. As shown elsewhere [26,27], the average current has the form

$$i_{tip} = \frac{i_0 t_0^n}{(1-n)\varepsilon_f^n} (\dot{\varepsilon}_{ct})^n \qquad \textbf{Eq. 2-28}$$

where $i_0$ is the bare surface current density, $t_0$ is the time of exposure of the bare surface prior to refilming, n is the current decay constant, $\varepsilon_f$ is the fracture strain of the passive film at the crack apex, and $\dot{\varepsilon}_{ct}$ is the crack tip strain rate. For the cyclic loading applied to Type 304 stainless steel, the crack tip strain rate can be estimated from the following equation [26].

$$\dot{\varepsilon}_{ct} = 145 f A_R (\Delta K)^4 \qquad \textbf{Eq. 2-29}$$

where $\Delta K$ is measured in MPa√m and

$$A_R = 2.44 \times 10^{-11} \quad \text{for } R \le 0.42$$

$$A_R = -2.79 \times 10^{-11} + 1.115 \times 10^{-10} R + 5.5 \times 10^{-11} R^2 \quad \text{for} \quad R > 0.42 .$$

R is the load ratio (= minimum load/maximum load).

Finally, the total rate of corrosion fatigue crack propagation, $V_{cr}$, can be presented as the sun of two parts

$$V = V_{el} + V_{mec} \qquad \textbf{Eq. 2-30}$$

where $V_{el}$ is the electrochemical component, which is determined by Faraday’s law [see Equation (2-19)], and $V_{mec}$ is the mechanical component (crack advance associated with mechanical fatigue/creep), which is determined by the equation [2-31]

$$V_{mec} = C\dot{\varepsilon}_{ct} \qquad \textbf{Eq. 2-31}$$

where *C* is a material constant.

Figures 2-3 and 2-4, which were obtained by using model kinetic parameters, show typical plots of crack growth rate as a function of the cyclic frequency for different values of corrosion potential, $E_{corr}$, and bulk concentration of NaCl. In performing these calculations, the kinetic parameters for the chemical and electrochemical reactions were taken from Ref. [21]. The geometrical mechanical parameters used in the calculation of corrosion fatigue propagation rate can be found in Table 2-1 and in the figure captions.

**Table 2-1**
**List of Geometrical and Mechanical Parameters**

| | | |
|---|---|---|
| L = 1 cm | $t_0$ = 0.01 s | E′ = 250 MPa |
| A = 2 cm | n = 0.5 | $\sigma_y$ = 160 Mpa |
| W = 6 cm | $\varepsilon_f = 8\times10^{-4}$ | $2\times10^{-2}$ cm |

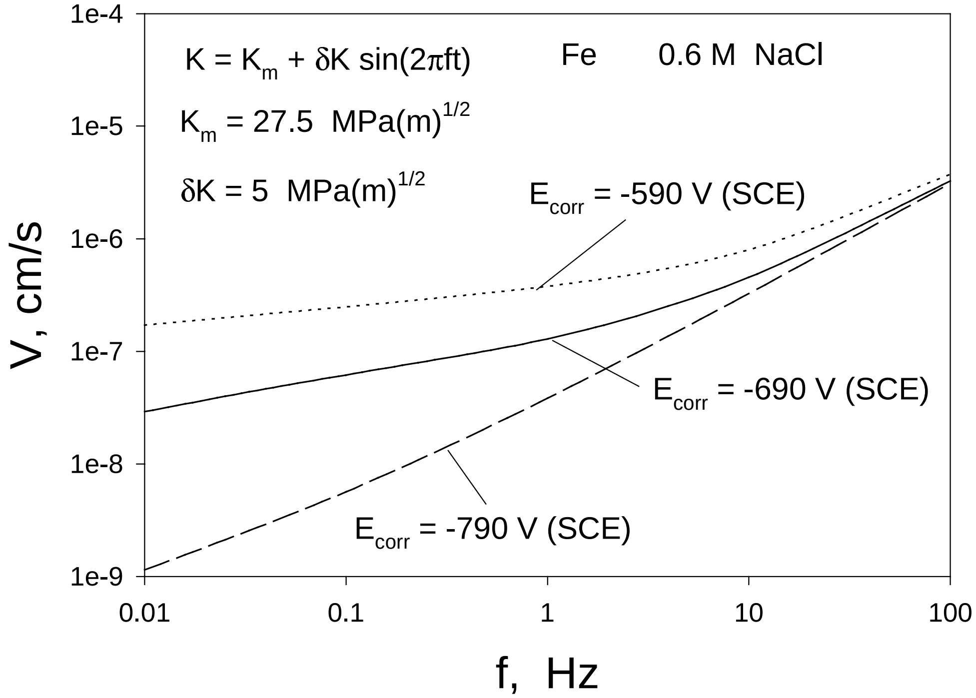

**Figure 2-3**
**The effect of loading frequency, f, on crack propagation rate for different corrosion potentials in 0.6 M NaCl with pH = 8 at T = 25 °C (77°F)**

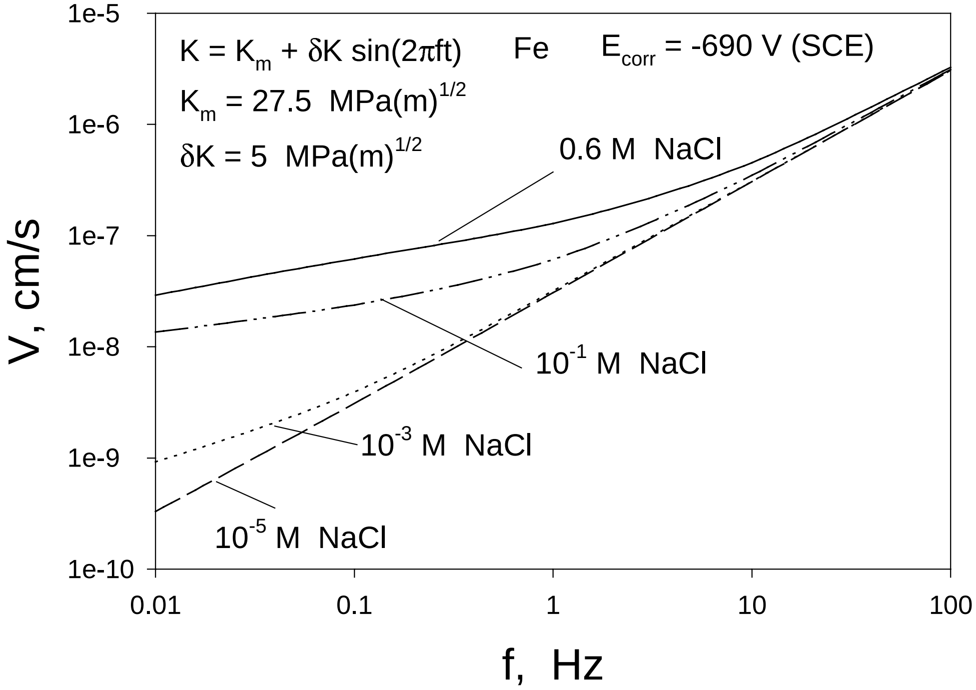

**Figure 2-4**
**The effect of loading frequency, f, on crack propagation rate for different bulk concentration of NaCl with pH = 8 at T = 25°C (77°F) and $E_{corr}$ = -690 V (SCE).**

These calculations are very time consuming and hence the numerical algorithms developed to date are not suitable for the final version of the code. Despite intense effort, we have not yet been able to develop simple, analytical expressions for estimating fatigue crack propagation rate. Development of such an expression is a pressing need, especially for the case of CF in steam turbines, where relatively high loading frequencies are experienced during operation.

In the absence of convection, the steady state conditions in the crevice can be classified according to the time constant

$$t_s = \frac{L^2}{D} \qquad \textbf{Eq. 2-32}$$

where D is the diffusion coefficient and L is the depth of the crack. Substituting $D = 10^{-5}$ cm$^2$ s$^{-1}$ and L = 1 mm into Equation (2-29), we obtain $t_s = 10^3$ s. Usually, for numerical calculations of this type, a time step, $\Delta t$, of the order of $0.01 \times t_s$ yields acceptable accuracy (i.e., approximately 100 steps are required to fulfill the calculation). However, if the stress intensity, $K_I$, is described by Equation (2-23), it is evident that the time step, $\Delta t$, must be an order of magnitude lower than 1/f. If f = 50 Hz ( STI Technologies has indicated a value of f = 600 Hz for one vibrational mode of the stress intensity), then $10 \times t_s/(1/f) = 5\ 10^5$ time steps are required to achieve steady state conditions. This means that the scope of the calculation increases by 2 - 3 order of magnitude for CF in comparison with SCC. It is important to note that $t_s \propto L^2$ and, if the depth of the cavity is increased to 1 cm, the scope of calculation will increase by an additional two order of magnitude. That is why there is a lack, in the current literature, of reported calculations of concentration and potential distributions in CF cracks for f >1-10 Hz.

Because a method for calculating the crack propagation rate, V, is going to be incorporated for CF into the algorithm for predicting the integral damage and because the simulation may require hundreds or perhaps thousand of individual calculations of V, the computational time must be markedly reduced. (Note that the algorithm must: (1) yield correct results and (2) have a reasonable execution time, or no one will use it). One way of dealing with problems of this nature is to introduce dimensionless variables (in order to reduce the number of independent variables), to calculate tables of dimensionless crack propagation rates as a function of these variables, and then to obtain the value of the real V by interpolation within these tables. For the case of active metal dissolution at the tip of a one-dimensional slot, this program has already been completed.

It can be shown that, for this case, the dimensionless tip concentration $C_S^* = C_{tip}/C_0$ is a function of dimensionless depth of the crack $L^* = L/L_0$ and the dimensionless parameter $\delta K/K$. Here, the following scales for the depth of the crack, $L_0$, and concentration, $C_0$, are introduced

$$L_0 = \sqrt{\frac{D}{2\pi f}} \quad \text{and} \quad C_0 = \frac{L_0 i_{tip}}{zFD} \qquad \textbf{Eq. 2-33}$$

Table 2-2 shows some results of numerical calculations. These calculated values of $C_S^*$ allow an immediate determination of the Nusselt number of the system, Nu, which for the case of a binary electrolyte and for the case when it is possible to neglect migration, yields a full description of the mass transfer conditions. Note that the dimensionless Nusselt number for mass transfer is defined by the equation

$$\frac{i_{tip}}{zF} = Nu \frac{DC_{tip}}{\tilde{L}} \qquad \textbf{Eq. 2-34}$$

where $\tilde{L}$ is the characteristic linear dimension of the system. If $\tilde{L} = L_0$ is chosen, it follows from Equations (2-33) and (2-34) that $Nu = 1/C_S^*$, i.e. $C_S^*$ is the reciprocal Nusselt number of the system. If more traditionally $\tilde{L} = L$ is chosen, we will have $Nu = \frac{L}{\sqrt{D/2\pi f}\, C_S^*}$. Of course, in more complicated cases some additional dimensionless parameters may be required.

**Table 2-2**
**Dimensionless Surface Concentrations, $C_S^*$, For Corrosion Fatigue in a One-Dimensional Slot.**

| $\delta K/K_m$ <br> $L^*$ | 0 | 0.1 | 0.25 | 0.5 | 1.0 |
|---|---|---|---|---|---|
| 0. | 0. | 0. | 0. | 0. | 0. |
| 6.0 | 6. | 3.35 | 4.82 | 5.40 | 5.80 |
| 60. | 60. | 9.24 | 22.1 | 35.2 | 50.2 |
| 300. | 300. | 20.1 | 50.2 | 89.8 | 158 |
| 600. | 600 | 30.2 | 74.9 | 138.2 | 252 |

Finally, it is noted that one of the alternative approaches for solving problems of the type faced in this program is to train an artificial neural network (ANN) on the time consuming numerical calculations and then use the ANN to perform the prediction of the corrosion fatigue crack growth rate in the code. This approach is also being explored and will be implemented if other approaches fail.

## 2.7 Algorithm for Predicting Integral Damage

In accordance with the theory developed above, calculation of the damage functions requires the determination of four independent functions for each kind of corrosion defect, k: The rate of defect nucleation, $n_k$, the defect growth rate, $V_k$, the delayed repassivation rate, $P_k$, and the rate of transition of one kind of defect to another, $R_k$, (for example, the transition of a pit into a crack). Accordingly, the algorithm for estimating the damage function must have at least four modules for handling these functions, but the operation of the algorithm is quite independent of the form of each function. Of course, additional modules are required for determining external parameters, such as the composition of the liquid film, temperature, corrosion potential, and so forth. A general algorithm together with a general modular computer code for predicting localized corrosion damage in steam turbines has been developed. The code contains five modules, as outlined in Figure 2-5.

**Damage Function Module** (DMF) is the main module of the code. To start calculations, it requires as input information about the initial distribution of damage, i.e. initial values for damage functions, $f_{k0}$. Sometimes, but not in the general case, it can simply be assumed that all $f_{k0}$ are equal zero (there is no initial damage in the system). Practically, the function of this module reduces to the numerical or analytical solution of the system of differential Equations for calculating the DF for all kinds of defects in the system. For each time step, this module calls the following four modules:

**Nucleation Module** (NM), which calculates the rate of defect nucleation, $n_k$, at the metal surface as a function of induction time;

**Growth Module** (GM), which computes the growth rate of corrosion events, $V_k$ as a function of its depth and, in the general case, at sufficiently small time steps if the external conditions depend on time;

**Repassivation Module** (RM), which calculates the rate of death of active events due to delayed repassivation;

**Transition Module** (TM), which compute the rate of transition (transformation) of one defect into another, $R_k$, as a function of population of defects, depth and, in the general case, observation time. It should be noted that RM can be regarded as a particular case of TM, because it also describes the transition of active events into their passive form and this passive form is a corrosion event in its own right. In order to emphasize this fact, RM and TM are combined in one block in Figure 2-5.

In turn, the four modules, NM, GM, RM, and TM, call the Environmental Module (EM) that defines the external conditions for the system, such as chemical composition, conductivity, and the thickness of the electrolyte film on the steel surface, corrosion potential, temperature, mechanical conditions, and so forth. In the general case, all parameters can depend on time (for example in the case of shutdowns and startups and transients during operation). At the moment, all of these parameters are assumed to be constant and known from experiment. However, after obtaining reliable electrochemical kinetic data for oxygen, hydrogen ion, and water reduction on the steam turbine steel, along with the value of the passive corrosion current density, the Mixed-Potential sub-Module (MPM) will be incorporated into the EM. This will calculate the corrosion potential of the turbine blades as a function of electrolyte composition, temperature, and electrolyte film thickness. MPM is based on the Wagner-Traud hypothesis for free corrosion processes and is customized for the case of general corrosion under thin electrolyte films and for the real electrochemical conditions that exist in a steam turbine. Many of the experimental data that are required for the MPM are currently being obtained at the Frumkin Institute (Moscow) in the parallel EPRI project, and will become available in the middle of 2001. The Chemistry sub-Module (CM) will also be incorporated into the EM. This will calculate the pH, composition, and conductivity of the external environment, as a function of the constraints [e.g., steam composition pressure and temperature.] The module will employ an equilibrium model, along with mass balance and charge balance constraints, to estimate species concentrations, and will compute ion activity coefficients using the extended Debye-Huckel theory. An alternative to the CM, if needed, could be the simple interpolation and extrapolation of experimental data that have been obtained or will be obtained in the parallel EPRI project at the Moscow Power Institute on relationships between the characteristics of inlet steam and the properties of the electrolyte films on the metal surfaces.

After determining the damage function for the system, the project will be in a position to address some important design questions. Thus, the output of the algorithm can be specified in three forms:

1. For a specified probability of failure, the algorithm can be used to estimate the damage function as a function of exposure time, and compute the observation time at which the depth of the deepest crack exceeds a *critical dimension.* The calculated observation time is the *service life*.

2. For a specified probability of failure and design life, the algorithm will calculate the *critical dimension* that can be tolerated to ensure acceptable performance.

For a specified wall thickness and design life, the algorithm could calculate the *failure probability*.

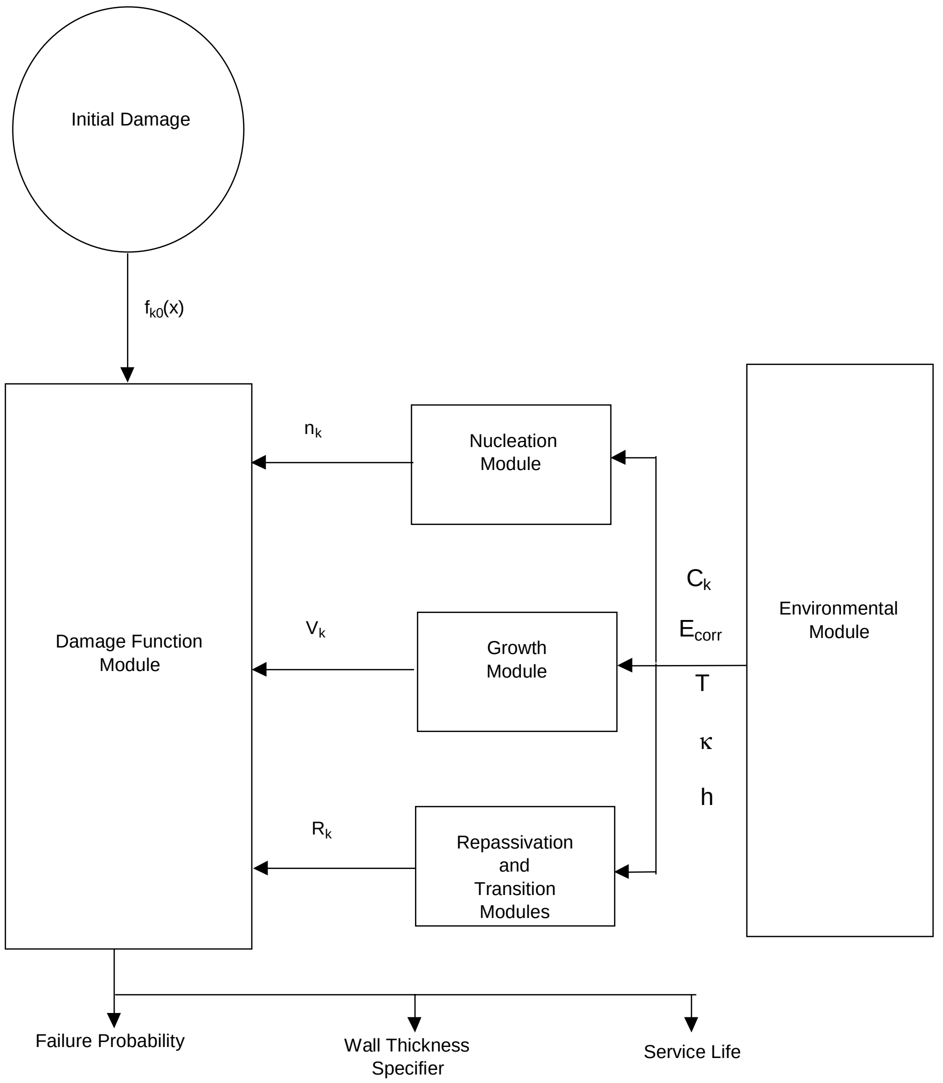

**Figure 2-5**
**Structure of algorithm for prediction of damage function**

# 3

# CONCLUSIONS

---

The principal results of this investigation to date can be summarized as follows:

1. A differential equation for calculating the damage function (DF) has been derived. By analytical or numerical solution of this equation it is possible to calculate DF in complicated systems with different corrosion events (active and passive pits, stress corrosion cracking, corrosion fatigue, etc.) if the rate of nucleation, rate of propagation, and probability of survival of the corrosion events are known.

2. A general mathematical model and corresponding computer code for calculating potential and concentration distributions in cavities for the cases of pitting corrosion, stress corrosion cracking (SCC), and corrosion fatigue (CF) have been developed. Mass transfer by diffusion, migration, and advection (fluid movement induced by the movement of the crack walls), anodic and cathodic processes at the crack tip and on the sides of the cavity, and hydrolysis and saturation solubility reactions is included in the model. The model also takes into account the potential drop in the external environment (outside the cavity).

3. On the basis of the general model, a simple, approximate, but nevertheless rather accurate, analytical model for calculating potential and concentration distributions along with cavity propagation rate has been developed for pitting corrosion and stress corrosion cracking. The model is based on the assumption that only those ionic species that are present at the highest concentrations in the crevice determine the potential distribution down the crack. The advantage of this method is that it permits simplification of the mathematics and allows one to predict the potential and concentration distributions without knowing various parameters, such as the equilibrium constants for homogeneous chemical reactions and the kinetic parameters for electrochemical reactions that do not significantly change the concentrations of principal ionic species in the cavity. The fact that reliable analytical expressions can be obtained for the rate of pit or crack propagation is very important, because the accurate numerical simulation of the evolution of localized corrosion damage over a long turbine-operating period may require a prohibitively large amount of computer time.

4. For the case of active metal dissolution at the tip of a one-dimensional slot under corrosion fatigue conditions, Nusselt numbers as a function of two dimensionless parameters have been calculated. For this particular case, the crack propagation rate can be quickly estimated by interpolation using these functions.

5. New criteria for the nucleation of stress corrosion and fatigue cracks from corrosion pits have been developed. Thus, it is shown that if the environmental component of the crack propagation rate is comparable with the mechanical (creep) component of the rate, the transition from a pit into a crack occurs if: (1) the depth of the pit exceeds some critical length (where stress intensity factor, $\Delta K$ exceeds the threshold stress intensity factor, $\Delta K_{tr}$), and (2) the pit is passivated.

6. General algorithms and computer codes for predicting localized corrosion damage in steam turbines have been developed.

# 4
# FUTURE WORK

Essentially the initial development of all prototype models required for predicting damage functions have been completed for the evolution of pitting and corrosion fatigue damage to low pressure steam turbine blades. However, as noted above, the code needs to be optimized to produce a tool that can be used to make damage predictions in a “user-friendly” manner and in execution times that are convenient for the operator. Accordingly the future work will emphasize code optimization, particularly with respect to predicting the accumulation of corrosion fatigue damage. Furthermore, many of the important parameter values that are being measured in parallel EPRI projects at Penn State University and at the Frumkin Institute in Moscow will not be available until mid 2001, so that the final touches to the algorithms must await receipt of these data. Specifically, it is proposed to:

- Greatly enhance the execution speed of the corrosion fatigue crack growth rate model by either developing analytical approximations or artificial neural networks, or both. Reduction of the execution time by a factor of $10^3$ to $10^4$ is the goal.
- Incorporate values for critically important model parameters that are now being measured at Penn State University and at the Frumkin Institute.
- Perform extensive dependent variable/independent variable sensitivity studies to ascertain the importance of individual processes and properties (e.g., electrolyte layer thickness and conductivity) in determining the rate of evolution of localized corrosion damage.
- Extensively compare the model predictions against laboratory and field data. Because none of these data are in the form of damage functions (c.f., Figure 1-2), the comparisons will have to be made with predictions of the individual models in the code (e.g., crack growth rate).
- Provide the optimized code to EPRI for incorporation into BLADE.

# 5

# SUPPORTING STUDIES

EPRI work in support of the present program is currently being carried out at the Pennsylvania State University and at the Frumkin Institute of Electrochemistry, Russian Academy of Sciences, Moscow, Russia. Both programs are designed to measure critically needed values for various model parameters for the Type 403 turbine blade stainless steel under conditions that are appropriate to steam turbine operation. These parameters include:

- Polarization data (including the passive current density) for the steel as a function of pH and $[Cl^-]$ at temperatures ranging from ambient (25°C, 77°F) to 200°C (392°F).
- Kinetic parameters for oxygen reduction and hydrogen evolution on the steel under similar conditions.
- Passivity breakdown parameters, including survival probability data for metastable pits
- Damage functions due to stable pitting, from which it is possible to calculate the delayed repassivation constant.

Particular attention is being paid to obtaining parameter values under demonstrably steady state conditions or in a manner that their inclusion in the code is justified by the constraints of the models. Details of this work will be published in separate EPRI reports.

# 6
# REFERENCES

---

1. O. Jonas, *Materials Performance*, 24, 9, (1985).
2. D. D. Macdonald and M. Urquidi-Macdonald, *Corrosion*, **48**, 354 (1992).
3. D. D. Macdonald, C. Liu, M. Urquidi-Macdonald, G. H. Sickford, B. Hindin, A. K. Agrawal, and K. Krist, *Corrosion*, **50**, 761 (1994).
4. G. Engelhardt, D. D. Macdonald and M. Urquidi-Macdonald, *Corros. Sci*., **41**, 2267 (1999).
5. G. Engelhardt and D. D. Macdonald, *Corrosion*, **54**, 469 - 479 (1998).
6. L. F. Lin, C. Y. Chao, and D. D. Macdonald, *J. Electrochem. Soc*., **128**, 1194 (1981).
7. D. D. Macdonald and M. Urquidi-Macdonald, *Electrochim. Acta*, **31**, 1079 (1986).
8. D. D. Macdonald and M. Urquidi-Macdonald, *J. Electrochem. Soc*., **134**, 41 (1987).
9. D. D. Macdonald and M. Urquidi-Macdonald, *J. Electrochem. Soc*., **136**, 961 (1989).
10. D. D. Macdonald and M. Urquidi-Macdonald, *J. Electrochem. Soc*., **139**, 3434 (1992).
11. G. Engelhardt and D. D. Macdonald. “The Deterministic Prediction of Localized Corrosion Damage in Aircraft Aluminum Alloys”. In 1998 USAF Aircraft Structural Integrity Program Conference, 1- 3 December 1998, San Antonio, Texas.
12. D.E. Williams, C. Westcott, and M. Fleischmann, *J. Electrochem. Soc.*, **132,** 1796, 1804 (1985).
13. U. Bertocci and Y. Yang-Xiang, *J. Electrochem. Soc.*, **131**, 1011 (1984).
14. G.S. Chen, K.-C. Wan, M. Gao, R. P. Wei and T. N. Flournoy, *Mat. Sci. Eng.*, **A219**, 126 (1996)
15. S. M. Sharland and P.W. Tasker, *Corros. Sci*. **28**, 603 (1988).
16. A. Turnbull and D. H. Ferris, *Corros. Sci.*, **27**, 1323 (1987).
17. Han En-Hou and Ke Wei, *Corros. Sci.,* **35**, 599 (1993).
18. A. Turnbull, Corros. Sci., **39**, 789 (1997).

19. D. D. Macdonald and M. Urquidi-Macdonald, *Corros. Sci.,* **32**, 51 (1991).

20. R. B. Dooley et al. Turbine Steam, Chemistry and Corrosion: Generation of Early Liquid Films in Turbines. EPRI, Palo Alto, CA. September 1999. TR-113090.

21. S. M. Sharland, C. P. Jackson and A. J. Diver, *Corros. Sci.,* 29, 1149 (1989).

22. A. Turnbull and D. H. Ferris, Corros. Sci., **27**, 1323 (1987).

23. Han En-Hou and Ke Wei, Corros. Sci., **35**, 599 (1993).

24. J. F. Knott, Fatigue Crack Growth – 30 Years of Progress, ed. R. A Smith, Pergamon Press, Oxford (1988).

25. A. Saxena and S. J. Hudak, Int. *J. Fract. Mech.,* **14**, 453 (1987).

26. F.P. Ford, and P.L. Andresen. Electrochemical Effects on Enviromentally –Assisted Cracking. In Parkins Symposium on Fundamental Aspects of Stress Corrosion Cracking, ed. S.M Bruemmer and al., TMS, 1992.

27. D. D. Macdonald, *Corros. Sci.,* **38**, 1003 (1996).

28. F.P. Ford, D.F. Tailor, P.L. Andresen, and R. G. Ballinger, Report NP-5064M, EPRI, Palo Alto, CA, 1987.

*Target:*

Boiler and Turbine Steam and Cycle Chemistry

## About EPRI

EPRI creates science and technology solutions for the global energy and energy services industry. U.S. electric utilities established the Electric Power Research Institute in 1973 as a nonprofit research consortium for the benefit of utility members, their customers, and society. Now known simply as EPRI, the company provides a wide range of innovative products and services to more than 1000 energy-related organizations in 40 countries. EPRI's multidisciplinary team of scientists and engineers draws on a worldwide network of technical and business expertise to help solve today's toughest energy and environmental problems.

EPRI. Electrify the World

© 2000 Electric Power Research Institute (EPRI), Inc. All rights reserved. Electric Power Research Institute and EPRI are registered service marks of the Electric Power Research Institute, Inc.
EPRI. ELECTRIFY THE WORLD is a service mark of the Electric Power Research Institute, Inc.

*Printed on recycled paper in the United States of America*

1000557

**SINGLE USER LICENSE AGREEMENT**

**THIS IS A LEGALLY BINDING AGREEMENT BETWEEN YOU AND THE ELECTRIC POWER RESEARCH INSTITUTE, INC. (EPRI). PLEASE READ IT CAREFULLY BEFORE REMOVING THE WRAPPING MATERIAL.**

BY OPENING THIS SEALED PACKAGE YOU ARE AGREEING TO THE TERMS OF THIS AGREEMENT. IF YOU DO NOT AGREE TO THE TERMS OF THIS AGREEMENT, PROMPTLY RETURN THE UNOPENED PACKAGE TO EPRI AND THE PURCHASE PRICE WILL BE REFUNDED.

**1. GRANT OF LICENSE**

EPRI grants you the nonexclusive and nontransferable right during the term of this agreement to use this package only for your own benefit and the benefit of your organization. This means that the following may use this package: (I) your company (at any site owned or operated by your company); (II) its subsidiaries or other related entities; and (III) a consultant to your company or related entities, if the consultant has entered into a contract agreeing not to disclose the package outside of its organization or to use the package for its own benefit or the benefit of any party other than your company.

This shrink-wrap license agreement is subordinate to the terms of the Master Utility License Agreement between most U.S. EPRI member utilities and EPRI. Any EPRI member utility that does not have a Master Utility License Agreement may get one on request.

**2. COPYRIGHT**

This package, including the information contained in it, is either licensed to EPRI or owned by EPRI and is protected by United States and international copyright laws. You may not, without the prior written permission of EPRI, reproduce, translate or modify this package, in any form, in whole or in part, or prepare any derivative work based on this package.

**3. RESTRICTIONS**

You may not rent, lease, license, disclose or give this package to any person or organization, or use the information contained in this package, for the benefit of any third party or for any purpose other than as specified above unless such use is with the prior written permission of EPRI. You agree to take all reasonable steps to prevent unauthorized disclosure or use of this package. Except as specified above, this agreement does not grant you any right to patents, copyrights, trade secrets, trade names, trademarks or any other intellectual property, rights or licenses in respect of this package.

**4. TERM AND TERMINATION**

This license and this agreement are effective until terminated. You may terminate them at any time by destroying this package. EPRI has the right to terminate the license and this agreement immediately if you fail to comply with any term or condition of this agreement. Upon any termination you may destroy this package, but all obligations of nondisclosure will remain in effect.

**5. DISCLAIMER OF WARRANTIES AND LIMITATION OF LIABILITIES**

NEITHER EPRI, ANY MEMBER OF EPRI, ANY COSPONSOR, NOR ANY PERSON OR ORGANIZATION ACTING ON BEHALF OF ANY OF THEM:

(A) MAKES ANY WARRANTY OR REPRESENTATION WHATSOEVER, EXPRESS OR IMPLIED, (I) WITH RESPECT TO THE USE OF ANY INFORMATION, APPARATUS, METHOD, PROCESS OR SIMILAR ITEM DISCLOSED IN THIS PACKAGE, INCLUDING MERCHANTABILITY AND FITNESS FOR A PARTICULAR PURPOSE, OR (II) THAT SUCH USE DOES NOT INFRINGE ON OR INTERFERE WITH PRIVATELY OWNED RIGHTS, INCLUDING ANY PARTY'S INTELLECTUAL PROPERTY, OR (III) THAT THIS PACKAGE IS SUITABLE TO ANY PARTICULAR USER'S CIRCUMSTANCE; OR

(B) ASSUMES RESPONSIBILITY FOR ANY DAMAGES OR OTHER LIABILITY WHATSOEVER (INCLUDING ANY CONSEQUENTIAL DAMAGES, EVEN IF EPRI OR ANY EPRI REPRESENTATIVE HAS BEEN ADVISED OF THE POSSIBILITY OF SUCH DAMAGES) RESULTING FROM YOUR SELECTION OR USE OF THIS PACKAGE OR ANY INFORMATION, APPARATUS, METHOD, PROCESS OR SIMILAR ITEM DISCLOSED IN THIS PACKAGE.

**6. EXPORT**

The laws and regulations of the United States restrict the export and re-export of any portion of this package, and you agree not to export or re-export this package or any related technical data in any form without the appropriate United States and foreign government approvals.

**7. CHOICE OF LAW**

This agreement will be governed by the laws of the State of California as applied to transactions taking place entirely in California between California residents.

**8. INTEGRATION**

You have read and understand this agreement, and acknowledge that it is the final, complete and exclusive agreement between you and EPRI concerning its subject matter, superseding any prior related understanding or agreement. No waiver, variation or different terms of this agreement will be enforceable against EPRI unless EPRI gives its prior written consent, signed by an officer of EPRI.

EPRI • 3412 Hillview Avenue, Palo Alto, California 94304 • PO Box 10412, Palo Alto, California 94303 • USA
800.313.3774 • 650.855.2121 • askepri@epri.com • www.epri.com